



Published in final edited form as:

Pediatr Res. 2018 June ; 83(6): 1218–1227. doi:10.1038/pr.2018.49.

Up-regulation of cholesterol 24-hydroxylase following hypoxia-ischemia in neonatal mouse brain

Fuxin Lu¹, Jun Zhu², Selena Guo³, Brandon J Wong⁴, Farid F. Chehab², Donna M. Ferriero^{1,5}, and Xiangning Jiang^{1,*}

¹Department of Pediatrics, University of California San Francisco, San Francisco, CA

²Department of Laboratory Medicine, University of California San Francisco, San Francisco, CA

³Dougherty Valley High School, San Ramon, CA

⁴University of California Berkeley, Berkeley, CA

⁵Department of Neurology, University of California San Francisco, San Francisco, CA

Abstract

Background—Maintenance of cholesterol homeostasis is crucial for brain development. Brain cholesterol relies on de novo synthesis and is cleared primarily by conversion to 24S-hydroxycholesterol (24S-HC) with brain-specific cholesterol 24-hydroxylase (CYP46A1). We aimed to investigate the impact of hypoxia-ischemia (HI) on brain cholesterol metabolism in the neonatal mice.

Methods—Postnatal day 9 C57BL/6 pups were subjected to HI using the Vannucci model. CYP46A1 expression was assessed by western blotting and its cellular localization was determined by immunofluorescence staining. The amount of brain cholesterol, 24S-HC in the cortex and in the serum was measured with ELISA.

Results—There was a transient cholesterol loss at 6hr after HI. CYP46A1 was significantly up-regulated at 6hr and 24hr following HI with a concomitant increase of 24S-HC in the ipsilateral cortex and in the serum. The serum levels of 24S-HC correlated with those in the brain, as well as with necrotic and apoptotic cell death evaluated by the expression of spectrin breakdown products and cleaved caspase-3 at 6hr and 24hr after HI.

Conclusions—Enhanced cholesterol turnover by activation of CYP46A1 represents disrupted brain cholesterol homeostasis early after neonatal HI. 24S-HC might be a novel blood biomarker for severity of hypoxic-ischemic encephalopathy with potential clinical application.

Users may view, print, copy, and download text and data-mine the content in such documents, for the purposes of academic research, subject always to the full Conditions of use:http://www.nature.com/authors/editorial_policies/license.html#terms

*Corresponding author: Xiangning Jiang, Department of Pediatrics, University of California, San Francisco 675 Nelson Rising Lane Room 494, San Francisco, CA 94158 Phone: 415-502-7278 Fax: 415-502-7325 xiangning.jiang@ucsf.edu.

Disclosure: The authors have no conflicts of interest and no financial relationships relevant to this article to disclose.

Introduction

Human brain cholesterol, which constitutes 25% of total body cholesterol, is crucial for brain development due to its importance in membrane integrity, myelination, synaptogenesis and neurotransmission (1, 2). The majority of brain cholesterol is stored in myelin sheaths, and the rest in the membranes of neurons, glial cells and other cellular elements. To accommodate rapid brain growth in the neonatal period, the rates of cholesterol biosynthesis and accretion are the greatest during this stage (first 3 weeks after birth in the rodents), a critical time for neuroplasticity, and then decline with age to reach a constant cholesterol level at adulthood (3–6). As cholesterol carried in lipoproteins in the blood cannot cross the blood brain barrier (BBB), brain cholesterol is produced exclusively from de novo synthesis (3, 7) using Acetyl-CoA as starting material and HMG-CoA reductase (HMGCR) as the rate-limiting enzyme. However, 24S-hydroxycholesterol (24S-HC), its metabolite that is generated through hydroxylation by cholesterol 24-hydroxylase (CYP46A1), is capable of traversing BBB and entering circulation to the liver for excretion (4, 7). CYP46A1 is brain-specific (4, 8), so most circulating 24S-HC has a cerebral origin (9). Thus the serum 24S-HC level could be an indication of brain cholesterol metabolism (10). In fact, plasma 24S-HC has been used as a surrogate marker of neuronal loss and brain atrophy in neurodegenerative diseases such as Alzheimer disease, Parkinson's disease and multiple sclerosis (11).

Cholesterol biosynthesis involves multiple enzymatic reactions and is an oxygen-consuming process that requires 11 oxygen molecules for the conversion of Acetyl-CoA to cholesterol (12). Therefore, cholesterol synthesis is sensitive to reduced O₂ availability and is limited in the conditions of hypoxia-ischemia (HI). This is evidenced by two studies in neonatal HI rats showing chronic loss of brain cholesterol lasting at least 3 days or 3 months following the insults (13, 14). Unfortunately, there are no additional investigations on the changes of cholesterol metabolism in response to HI in the immature brain and the underlying mechanisms. Recent in vitro studies suggest that oxidative stress (6) and endogenous neurotransmitters upregulate CYP46A1, with glutamate eliciting the highest increase in CYP46A1 activity (15). These are well-accepted mechanisms that are associated with brain damage in neonatal hypoxic-ischemic encephalopathy (HIE), the clinical syndrome of brain dysfunction in the newborns with few tools for diagnosis and intervention (16). Studies on regulation of cholesterol homeostasis in the developing brain, as well as its disturbance after HI at early postnatal stage, would allow for a better understanding of lipid disorders and their involvement in HIE gray and white matter injury.

The present study focused on the responses of cholesterol metabolism after neonatal HI in postnatal day 9 (P9) mice, an age equivalent to full term human infants. We hypothesized that the brain-specific cholesterol hydroxylase, CYP46A1, is activated following neonatal HI leading to an enhanced production of 24S-HC in the brain, and in the circulation. Herein, we demonstrated an increase and correlation of the 24S-HC levels in the serum and in the brain, and importantly, a significant positive correlation between serum 24S-HC levels and cortical injury evaluated by the expression of spectrin breakdown products (SBDPs) and cleaved caspase-3, representing activation of necrosis and/or apoptosis, at 6hr and 24hr after HI. These findings suggested a possibility of using 24S-HC as a potential blood biomarker for severity of HIE brain injury.

Methods

All animal experiments were approved by the University of California San Francisco institutional animal care and use committee. C57BL/6 mice (Charles River Laboratory, Hollister, CA) with litters were allowed food and water *ad libitum*. Both sexes were used on P9.

Neonatal Brain Hypoxia-Ischemia

Neonatal HI was performed using the Vannucci model. On P9, the pups underwent left common carotid artery (CCA) coagulation through a vertical midline neck incision under isoflurane anesthesia (2–3% isoflurane, balanced oxygen) to induce unilateral ischemia. The animals were recovered for one hour with their dam and then exposed to 60 minutes of hypoxia in a humidified chamber at 37°C with 10% oxygen/balanced nitrogen to induce global hypoxia. Sham-operated control animals received isoflurane anesthesia and exposure of the left CCA without coagulation and hypoxia. The animals were dissected immediately after hypoxia (0hr) or returned to their dams until they were euthanized at 1hr, 6hr, 24hr, 48hr or 72hr after the procedure.

Sample preparation

The cortices were dissected and quickly sliced into small pieces on ice, mixed and divided into 3 equal fractions for protein (western blotting), cholesterol or 24S-HC measurements respectively. For protein purification, the tissue was homogenized in radioimmunoprecipitation assay (RIPA) buffer (R0278, MilliporeSigma, Temecula, CA) with protease and phosphatase inhibitors followed by centrifugation at 14,000 rpm for 15 mins. The supernatant was saved and the protein concentration was measured with BCA kit (Pierce Biotechnology, Rockford, IL). For 24S-HC assay, the tissue was sonicated with 95% ethanol, after centrifugation at 7,000 ×g for 5 mins, the supernatant (A) was collected and the pellet was sonicated again in the extract buffer (ethanol: dichloromethane (1:1; v/v)) followed by centrifugation at 7,000 ×g for 5 mins. The resultant supernatant (B) was combined with supernatant A and dried with speed vacuum. The dried pellet was rehydrated by adding 8μl of 95% ethanol and 242μl of assay buffer 40 (24S-Hydroxycholesterol ELISA Kit, ab204530, Abcam, Cambridge, MA). For cholesterol measurement, the tissue was extracted with 200μl of chloroform: isopropanol: IGEPAL CA-630 (7:11:0.1) in a microhomogenizer and spun at 13,000 ×g for 10 mins to remove insoluble material. The organic phase was air-dried at 50°C for 15 mins to remove chloroform. The samples were then dried with speed vacuum and dissolved in 200μl cholesterol assay buffer (Cholesterol Quantitation Kit, MAK043, MilliporeSigma) for cholesterol quantification.

Serum was collected from the same animals using BD SST microtainer capillary blood collection tube with serum separator (#365967, BD, Franklin Lakes, NJ).

Western blotting

An equal amount of protein samples (40μg) was applied to 4–12% Bis-Tris SDS polyacrylamide gel electrophoresis and transferred to polyvinylidene difluoride membrane at 30V overnight at 4°C. After blocking with TBS containing 0.05% Tween 20 (TBST) buffer

with 5% milk for 1 hour, the blots were probed overnight at 4°C with the following primary antibodies: anti-cholesterol-24-hydroxylase 1A7 (1:500; MAB2259, MilliporeSigma); anti- α -spectrin (1:5000, MAB1622, MilliporeSigma); anti-cleaved caspase-3 (1:1000, # 9664, Cell Signaling Technology Inc.; CST; 3 Trask Lane, Danvers, MA) and anti- β -actin (1:5000, sc-47778, Santa Cruz Biotechnology Inc., Santa Cruz, CA). Appropriate secondary HRP-conjugated antibodies (Santa Cruz) were used. The protein signal was visualized with enhanced chemiluminescence and developed with radiographic film. Image J software was used to measure the mean optical densities (OD) and areas of protein signal on the film after scanning.

Enzyme-linked immunosorbent assay for 24S-HC levels in the cortex and serum

A competitive ELISA kit (ab204530, Abcam) was used to measure the levels of 24S-HC in the cortex and serum. A fresh set of 24S-HC standard was prepared at a range of 0.39ng/ml to 100ng/ml and a clear 96 well plate coated with goat anti-rabbit IgG was used. Briefly, 100 μ l of standards and samples were pipetted into the appropriate wells. 50 μ l of the diluted biotin-labeled 24S-HC conjugate was then added to each well except for the blanks. 50 μ l of the rabbit 24S-HC antibody that can bind to either 24S-HC in the samples or to the labeled 24S-HC conjugate was added to each well except for the blanks and the nonspecific binding (NSB) wells. The plate was incubated for 1 hour at RT. After washing 4 times with 400 μ l of wash buffer, 200 μ l of streptavidin-HRP solution was pipetted into each well to bind to biotin-labeled 24S-HC conjugate. The plate was incubated for 30 mins at RT. After the 2nd wash, 200 μ l of 3,3',5,5'-Tetramethylbenzidine (TMB) substrate solution was added and incubated at RT for 30 mins. To stop the reaction, 50 μ l of stop solution (1N HCl) was added and the absorbance (optical density, OD) was read at 450nm with a microplate reader (BioTek Synergy HT). The intensity of signal was inversely proportional to the levels of 24S-HC in the samples. For each standard and sample, the net OD = OD-NSB OD. A standard curve was made for the calculation of the levels of 24S-HC. The concentration of cortical 24S-HC was normalized to the wet weight of the starting tissue (ng/mg wet weight). The concentration of serum 24S-HC was normalized to the serum protein concentration (ng/mg protein).

Cholesterol measurement

A cholesterol quantitation kit (MAK043, MilliporeSigma) was used to measure the concentration of cholesterol in the cortex. The samples prepared above were diluted at 1:10 with assay buffer and seven cholesterol standards (0.02 μ g/ μ l to 0.14 μ g/ μ l) were prepared. 100 μ l of standards and samples were pipetted into the appropriate wells of a clear 96 well plate. 50 μ l of reaction mix buffer including cholesterol probe, cholesterol enzyme mix and cholesterol esterase was added to each well. The plate was incubated at 37°C for 60 mins protected from light. The absorbance was read at 570nm and the concentration of cholesterol in the samples was calculated using the standard curve. The levels of cortical cholesterol were normalized to the wet weight of the starting tissue (μ g/mg wet weight).

Immunofluorescent staining

At 24hr after HI, the sham and injured mice were perfuse-fixed with 4% paraformaldehyde (PFA) in 0.1mol/L phosphate buffer (pH 7.4). Brains were dissected and post-fixed in 4%

PFA overnight at 4°C, and then transferred to 30% sucrose in 0.1 mol/L phosphate buffer for cryoprotection for 3 days. The brains were embedded in O.C.T compound and cryosections were cut at 16µm. The sections were defrosted and air-dried at RT for 2 hrs. After washing with PBS, sections were boiled in 0.01M sodium citrate buffer (pH 6.0, with 0.05% Tween 20) at 90°C for 30 mins to retrieve antigen. After washing with PBS, the sections were blocked with blocking buffer (10% goat serum and 0.1% Triton X-100 in PBS) for 1 hr and then incubated overnight at 4°C with mouse anti-CYP46A1 antibody (1:50, MAB2259, MilliporeSigma), paired with another rabbit antibody that labels different cell types: anti-NeuN for neurons (1:500, #ab177487, Abcam); or anti-GFAP for astrocytes (1:500, #Z0334, Dako, Santa Clara, CA); or anti-Iba1 for microglia (1:1000, #019-19741, Wako Chemicals, Richmond, VA); or anti-MBP for oligodendrocytes (1:200, #78896, CST). Antibody against cleaved caspase-3 (1:500, #9664, CST) was used for double staining with anti-CYP46A1 to study their co-localization. After washing with 0.025% Tween/PBS for 3 times, the sections were incubated with goat anti-mouse Alexa Fluor 568 (1:500; # A-11004, Invitrogen, Grand Island, NY) and goat anti-rabbit Alexa Fluor 488 (1:500, #A-11034, Invitrogen) for 1hr at RT and exposed to DAPI for 5 min and then cover-slipped with ProLong Diamond antifade reagent (Invitrogen). Images were taken with Leica TCS SP5 Spectral Confocal Microscope.

Statistical Analysis

SAS Wilcoxon-Mann-Whitney test was used to evaluate the OD values of protein expression in Western blotting, brain concentrations of cholesterol, and the cortical and serum levels of 24S-HC. Pearson's correlation coefficient analysis was used to evaluate the correlation between cortical and serum levels of 24S-HC, and between serum 24S-HC and protein levels of spectrin breakdown product (SBDP) at 145/150KDa, SBDP at 120KDa, or cleaved caspase-3. Differences were considered significant at $p < 0.05$.

Results

Up-regulation of CYP46A1 with a concomitant increase of 24S-HC in the brain following neonatal HI

To investigate how cholesterol metabolism is impacted by neonatal HI, we measured the protein expression of CYP46A1, the enzyme responsible for elimination of excess cholesterol from the brain, at various post-HI time points for up to 3 days. As shown in Fig. 1A, CYP46A1 was significantly upregulated at 6hr and 24hr after HI compared to the sham animals at the same time points, and declined at 48hr and 72hr (sham vs. HI: $p = 0.0339$ at 6hr; $p = 0.0026$ at 24hr; $n = 5-6$ for sham animals, $n = 6-12$ for HI animals at 6-72hr). The increased expression of CYP46A1 was confirmed by immunofluorescent staining with anti-CYP46A1 antibody at 24hr after HI, when the fluorescent intensity was much higher in the ipsilateral cortex compared to that of the sham animals and the contralateral hemisphere (left panels in Fig. 1B). It is interesting that the expression of CYP46A1 in the ipsilateral cortex was largely localized to the cells undergoing apoptotic cell death as visualized by the expression of cleaved caspase-3 (Fig. 1B).

The pattern of 24S-HC levels in the ipsilateral cortex was similar to that of CYP46A1 expression with a marked increase at 6 and 24hr post-HI compared to that of the sham

controls (Fig. 1C, sham vs. HI: $p=0.0167$ at 6hr; $p=0.0085$ at 24hr; $n=3-6$ for sham animals, $n=5-7$ for HI animals at 6–72hr). At 6hr, 24S-HC in the ipsilateral cortex was higher than that in the contralateral side, too (Fig. 1C, HI ipsi vs. HI contra: $p=0.0493$ at 6hr). HI-induced over-production of 24S-HC in the ipsi-cortex sustained at 48hr although the difference was not statistically significant compared to that of the sham animals (Fig. 1C, sham vs. HI: $p=0.0526$ at 48hr). There was a trend of more 24S-HC produced in the contralateral cortex (underwent hypoxia) at 6 and 24hr, but the differences were not significant (Fig. 1C, right panel). These results demonstrated that the up-regulated CYP46A1 was functional, which led to robust cholesterol turnover early after HI, along with an enhanced production of its metabolic product 24S-HC in the injured cortex, but not in the non-injured contralateral hemisphere.

To determine whether the increased cholesterol metabolism following neonatal HI would diminish brain cholesterol amount, we measured cholesterol levels in the sham and HI-injured ipsi- and contra-lateral cortex at the same time points. We found a significant, but transient loss of cholesterol at 6hr after HI in the ipsilateral cortex (Fig. 2A, sham vs. HI ipsi: $p=0.0304$ at 6hr; $n=7$), but not in the contralateral side (sham vs. HI contra: $p=0.1736$; $n=7$) compared to the sham animals. This change represented the net results of de novo cholesterol synthesis and turnover. The enhanced cholesterol hydroxylation/breakdown may, at least in part, contribute to the cholesterol loss at 6hr, whereas the elevated expression of HMGCR, the rate-limiting enzyme for cholesterol biosynthesis, at 24hr (Fig. 2B, 2C, sham vs. HI: $p=0.047$ at 24hr, $n=3-11$) indicates feedback mechanisms for replenishment and re-establishment of cholesterol balance at 24hr and the time points thereafter.

Expression of CYP46A1 in neurons and oligodendrocytes

CYP46A1 was originally reported to be neuron-specific, however, several recent studies demonstrated its presence in glial cells, including microglia and astrocytes in different injury paradigms (17, 18). To study the cellular localization of CYP46A1 in our neonatal HI model, we stained the brain sections from the sham and injured pups (at 24hr post-HI) with CYP46A1 antibody paired with another antibody specific for neuron (NeuN), astrocyte (GFAP), oligodendrocyte (MBP) or microglia (Iba1). Fig. 3 indicated that the enzyme was expressed in neurons (shown in the cortical region) and oligodendrocytes (OLGs, shown in the corpus callosum) in both sham (Fig. 3A) and the injured animals (Fig. 3B). Co-localization was not found in the astrocytes and microglia in the sham (not shown) and injured brains (Fig. 3B). The CYP46A1 staining was in the cytoplasm.

Correlation of the 24S-HC levels in the serum and in the brain after neonatal HI

As CYP46A1 converts brain cholesterol to the more soluble 24S-HC, which readily crosses BBB, and this enzymatically-generated oxysterol is specifically made in the brain, we asked whether there is an efflux of 24S-HC from the brain into the periphery circulation after HI. We measured the serum levels of 24S-HC and evaluated its relationship with brain levels. In line with the increased production in the brain, there was a boost of serum 24S-HC levels at 6hr after HI, which sustained for 48hr before returning to the sham values at 72hr (Fig. 4A, sham vs. HI, $p=0.0102$ at 6hr; $p=0.0046$ at 24hr; $p=0.0167$ at 48hr; $n=3-6$ for sham animals, $n=5-13$ for HI animals at 6–72hr). There was a strong correlation of 24S-HC levels in the

serum and in the ipsilateral cortex (Fig. 4B, $R^2=0.521$, $p<0.0001$, $n=40$) implicating the brain as the major source of circulating 24S-HC (note that the concentrations of 24S-HC in the serum were normalized to serum protein concentrations as ng/mg protein, whereas in the brain they were normalized to the tissue wet weight as ng/mg wet weight).

Correlation of serum 24S-HC levels with brain injury at 6hr and 24hr after HI

Since cholesterol is essential for membrane and myelin integrity, CYP46A1 upregulation may cause membrane disruption or myelin breakdown leading to cell death and brain injury after HI. We hypothesized that increased serum 24S-HC values could forecast HI-induced cell loss and gray/white matter damage. We assessed acute brain injury within 3 days with the protein expression of spectrin breakdown products (SBDP) at 145/150 KD and 120KD representing activation of necrosis and/or apoptosis, as well as the cleaved caspase-3 indicating apoptotic cell death. The expression of both SBDP at 145/150KD and 120KD considerably increased at 6hr and 24hr after HI compared to the sham animals (Fig. 5A, for SBDP145/150KD, sham vs. HI, $p=0.0094$ at 6hr, $p=0.0013$ at 24hr. For SBDP120KD, sham vs. HI, $p=0.036$ at 6hr, $p=0.0087$ at 24hr. $n=4-6$ for sham animals, $n=6-15$ for HI animals from 6-72hr). The increase in cleaved caspase-3 levels lasted longer for 48hr and subsided at 72hr (Fig. 6A, sham vs. HI, $p=0.0112$ at 6hr; $p=0.0027$ at 24hr; $p=0.0228$ at 72hr, $n=5-6$ for sham animals, $n=7-10$ for HI animals from 6-72hr). There was a positive correlation between serum 24S-HC levels and SBDP 145/150KD at 6hr and 24hr post-HI (Fig. 5B, at 6hr: $R^2=0.713$, $p=0.002$, $n=10$; at 24hr: $R^2=0.656$, $p=0.003$, $n=11$); and with cleaved caspase-3 at the same time points (Fig. 6B, at 6hr: $R^2=0.738$, $p=0.002$, $n=10$; at 24hr: $R^2=0.462$, $p=0.044$, $n=9$). The correlation between serum levels of 24S-HC and SBDP120 KD was also significant at 24hr (Fig. 5B, $R^2=0.557$, $p=0.008$, $n=11$).

Discussion

We demonstrated an enhanced brain cholesterol turnover following neonatal hypoxia-ischemia as evidenced by the up-regulation of CYP46A1 in the ipsilateral cortex, leading to an increased production of 24S-HC in the injured hemisphere and simultaneous excretion into the bloodstream. The correlation between the levels of serum 24S-HC and brain necrosis/apoptosis at early post-HI stage supports a possible value of plasma level of 24S-HC as a novel and early biomarker for severity of neonatal HI brain damage.

Present mainly in the brain, CYP46A1 catalyzes the hydroxylation of cholesterol into 24S-HC to eliminate surplus cholesterol from the brain, and thereby plays an important role in maintenance of cholesterol homeostasis (19, 20). CYP46A1 protein expression is low before 1 week after birth in mice and gradually increases to reach a steady level around 3 weeks (6, 8). In humans, it reaches the adult level around 3 years old (8). This allows deposition of nearly all cholesterol at an early age to assist in the rapid expansion of the brain and myelin, and in the removal of redundant cholesterol as the animal matures. We showed an upregulation of CYP46A1 following neonatal HI at P9 sustaining at least 24 or 48hrs. It is unknown how this enzyme is activated by hypoxia-ischemia, whether this response is simply adaptative, or is it involved in processes of brain injury or protection. CYP46A1 promoter activity appears to be resistant to changes of molecules implicated in regulation of

cholesterol homeostasis including cholesterol and 24S-HC (6), but can be induced by the Sp-family of transcriptional factors (21) and epigenetic modifications (22). Recent studies have suggested two mechanisms for CYP46A1 activation: oxidative stress (6) and glutamate (15), both of which are associated with cell death in brain ischemia, and with overactivation of the NMDA receptors (NMDARs), the major ionotropic glutamate receptors mediating excitotoxicity in HI brain injury. CYP46A1 enzymatic product 24S-HC was found to be a potent allosteric modulator to enhance the function of NMDARs (23, 24). These findings suggest a reciprocal activation of the NMDAR pathway and the cholesterol metabolism pathway, which may form a vicious cycle to exacerbate brain damage following neonatal HI.

Cholesterol loss is expected to be the direct consequence of CYP46A1 activation. This might be partially responsible for the reduction in cholesterol in the ipsilateral cortex at 6hr after HI. The changes of total cholesterol amount found here reflected the balance between de novo synthesis and breakdown by CYP46A1. We did not measure cholesterol that was newly synthesized after neonatal HI. However, elevated generation of 24S-HC could down-regulate cholesterol synthesis via blocking the proteolytic activation of transcription factor sterol regulatory element-binding protein 2 (SREBP2), which controls the pathway of cholesterol biosynthesis (25). In connection with excitotoxicity, a Ca²⁺-dependent cholesterol loss was found in cultured hippocampal neurons exposed to NMDA, which was paralleled by translocation of CYP46A1 from the endoplasmic reticulum, where it normally resides, to the plasma membrane and release of 24S-HC into the medium (26). Apparently, we cannot draw the conclusion that cholesterol loss at 6hr was solely attributable to the action of CYP46A1. The level of HMGCR was unchanged at 6hr, but increased at 24hr after HI, which might prevent further reduction of cholesterol in the injured hemisphere. The other two studies of neonatal HI in P7 SD rats also reported the diminished cholesterol contents, which lasted longer for 3 days or 3 months following the initial insult (13, 14). Disturbance of cholesterol homeostasis after neonatal HI may have adverse consequences on cell survival and brain development. For example, accelerated cholesterol hydroxylation found in this study produced a high level of 24S-HC, which has been shown to be cytotoxic to neurons by inducing apoptosis, necroptosis (a form of programmed necrosis) (27, 28), inflammatory responses (29) and cognitive impairment (30). The co-localization of increased CYP46A1 with cleaved caspase-3 in the ipsilateral cortex indicates that CYP46A1 may be associated with cell death following HI. Further studies are required to elucidate the functional roles of CYP46A1 and 24S-HC in neonatal brain hypoxia-ischemia, especially in long-term neurological deficits.

Although primarily confined to neurons in the healthy brain, CYP46A1 has been found in other cell types in different disease conditions, for example, in activated microglia and reactive astrocytes in brain trauma (17, 18), in astrocytes of Alzheimer disease patients (31), or in macrophages/microglia in an animal model of multiple sclerosis (32). They were proposed to clear extracellular cholesterol released from the damaged cell membranes, which has not been proved experimentally. We show that CYP46A1 is localized in neurons and oligodendrocytes, but not in astrocytes and microglia. White matter is a common lesion site in rodent neonatal HI (33) and in human infants, especially preterm babies (34), who suffered from HIE. As oligodendrocytes are sensitive to oxidative stress and excitotoxicity in

the developing brain (35), if CYP46A1 is up-regulated in oligodendrocytes after HI, it may break down cholesterol leading to myelin degradation or limiting its availability for myelin synthesis and white matter development as cholesterol in oligodendrocytes is a rate-limiting factor for brain maturation (2). Targeted inhibition or deletion of CYP46A1 in oligodendrocyte may reveal its precise function in normal brain and in disease conditions. Different cell populations play distinct roles in regulating cholesterol homeostasis. For example, neurons can utilize external cholesterol transported from glial cells (36, 37). Similarly, brain cells may coordinate for cholesterol clearance because not all brain cells; even not all neurons, express CYP46A1 (8, 20).

Studies with CYP46A1 knockout mice have suggested that this enzyme is responsible for the production of \approx 98–99% of brain 24S-HC and \approx 60–80% 24S-HC in the serum (9, 38). Our data support the cerebral origin of blood 24S-HC owing to the concomitant increase and correlation of 24S-HC in the serum and in the brain. Although it is unknown whether an acute elevation of serum 24S-HC can predict histological and functional outcomes at later time points, based on its brain specificity, and a strong correlation with necrotic and apoptotic cell death early after HI, this pilot work suggests that blood 24S-HC might be a biologically plausible marker for HIE to assist clinical diagnosis. SBDP can be detected in the serum of human neonates and the amounts are associated with the severity of HIE clinical syndromes with good sensitivity and specificity (39). However, serum SBDP can be derived from extracerebral organs when damaged. Radiological or functional measures are needed to explore the feasibility of using blood 24S-HC as a diagnostic tool in HIE patients. Targeted lipid profiling discovered plasma sphingomyelins as potential markers for acute stroke patients (40). Lipids could be better tools for diagnosis than protein markers due to their abundance in the brain, small size for readily crossing the BBB, and higher sensitivity to oxidative stress for a possible earlier detection.

Taken together, this is the first study investigating a brain-specific cholesterol turnover pathway following neonatal hypoxia-ischemia. Activation of CYP46A1 may play more specialized roles than just removing cholesterol from the central nervous system. Future work is required to gain better insight into cholesterol homeostasis in the developing brain, which is subject to a more sophisticated regulation than that in the adult brain where cholesterol is largely metabolically inert.

Acknowledgments

Statement of financial support: This work was supported by the National Institute of Neurological Disorders and Stroke (RO1NS084057 to Dr. Jiang).

References

1. Mauch DH, Nagler K, Schumacher S, et al. CNS synaptogenesis promoted by glia-derived cholesterol. *Science*. 2001; 294:1354–7. [PubMed: 11701931]
2. Saher G, Brugger B, Lappe-Siefke C, et al. High cholesterol level is essential for myelin membrane growth. *Nat Neurosci*. 2005; 8:468–75. [PubMed: 15793579]
3. Dietschy JM. Central nervous system: cholesterol turnover, brain development and neurodegeneration. *Biol Chem*. 2009; 390:287–93. [PubMed: 19166320]

4. Dietschy JM, Turley SD. Thematic review series: brain Lipids. Cholesterol metabolism in the central nervous system during early development and in the mature animal. *J Lipid Res.* 2004; 45:1375–97. [PubMed: 15254070]
5. Quan G, Xie C, Dietschy JM, Turley SD. Ontogenesis and regulation of cholesterol metabolism in the central nervous system of the mouse. *Brain Res Dev Brain Res.* 2003; 146:87–98. [PubMed: 14643015]
6. Ohyama Y, Meaney S, Heverin M, et al. Studies on the transcriptional regulation of cholesterol 24-hydroxylase (CYP46A1): marked insensitivity toward different regulatory axes. *J Biol Chem.* 2006; 281:3810–20. [PubMed: 16321981]
7. Jurevics H, Morell P. Cholesterol for synthesis of myelin is made locally, not imported into brain. *J Neurochem.* 1995; 64:895–901. [PubMed: 7830084]
8. Lund EG, Guileyardo JM, Russell DW. cDNA cloning of cholesterol 24-hydroxylase, a mediator of cholesterol homeostasis in the brain. *Proc Natl Acad Sci U S A.* 1999; 96:7238–43. [PubMed: 10377398]
9. Bjorkhem I, Lutjohann D, Diczfalusy U, Stahle L, Ahlborg G, Wahren J. Cholesterol homeostasis in human brain: turnover of 24S-hydroxycholesterol and evidence for a cerebral origin of most of this oxysterol in the circulation. *J Lipid Res.* 1998; 39:1594–1600. [PubMed: 9717719]
10. Lutjohann D, von Bergmann K. 24S-hydroxycholesterol: a marker of brain cholesterol metabolism. *Pharmacopsychiatry.* 2003; 36(Suppl 2):S102–6. [PubMed: 14574622]
11. Leoni V, Caccia C. 24S-hydroxycholesterol in plasma: a marker of cholesterol turnover in neurodegenerative diseases. *Biochimie.* 2013; 95:595–612. [PubMed: 23041502]
12. DeBose-Boyd RA. Feedback regulation of cholesterol synthesis: sterol-accelerated ubiquitination and degradation of HMG CoA reductase. *Cell Res.* 2008; 18:609–21. [PubMed: 18504457]
13. Ramirez MR, Muraro F, Zylbersztejn DS, et al. Neonatal hypoxia-ischemia reduces ganglioside, phospholipid and cholesterol contents in the rat hippocampus. *Neurosci Res.* 2003; 46:339–47. [PubMed: 12804795]
14. Yu Z, Li S, Lv SH, et al. Hypoxia-ischemia brain damage disrupts brain cholesterol homeostasis in neonatal rats. *Neuropediatrics.* 2009; 40:179–85. [PubMed: 20146174]
15. Mast N, Anderson KW, Johnson KM, Phan TTN, Guengerich FP, Pikuleva IA. In vitro cytochrome P450 46A1 (CYP46A1) activation by neuroactive compounds. *J Biol Chem.* 2017; 292:12934–46. [PubMed: 28642370]
16. Millar LJ, Shi L, Hoerder-Suabedissen A, Molnar Z. Neonatal Hypoxia Ischaemia: Mechanisms, Models, and Therapeutic Challenges. *Front Cell Neurosci.* 2017; 11:78. [PubMed: 28533743]
17. Cartagena CM, Ahmed F, Burns MP, et al. Cortical injury increases cholesterol 24S hydroxylase (Cyp46) levels in the rat brain. *J Neurotrauma.* 2008; 25:1087–98. [PubMed: 18729719]
18. Smiljanic K, Lavrnja I, Mladenovic Djordjevic A, et al. Brain injury induces cholesterol 24-hydroxylase (Cyp46) expression in glial cells in a time-dependent manner. *Histochem Cell Biol.* 2010; 134:159–69. [PubMed: 20559650]
19. Moutinho M, Nunes MJ, Rodrigues E. Cholesterol 24-hydroxylase: Brain cholesterol metabolism and beyond. *Biochim Biophys Acta.* 2016; 1861:1911–20. [PubMed: 27663182]
20. Russell DW, Halford RW, Ramirez DM, Shah R, Kotti T. Cholesterol 24-hydroxylase: an enzyme of cholesterol turnover in the brain. *Annu Rev Biochem.* 2009; 78:1017–40. [PubMed: 19489738]
21. Milagre I, Nunes MJ, Gama MJ, et al. Transcriptional regulation of the human CYP46A1 brain-specific expression by Sp transcription factors. *J Neurochem.* 2008; 106:835–49. [PubMed: 18445135]
22. Shafaati M, O'Driscoll R, Bjorkhem I, Meaney S. Transcriptional regulation of cholesterol 24-hydroxylase by histone deacetylase inhibitors. *Biochem Biophys Res Commun.* 2009; 378:689–94. [PubMed: 19059217]
23. Linsenbardt AJ, Taylor A, Emnett CM, et al. Different oxysterols have opposing actions at N-methyl-D-aspartate receptors. *Neuropharmacology.* 2014; 85:232–42. [PubMed: 24878244]
24. Paul SM, Doherty JJ, Robichaud AJ, et al. The major brain cholesterol metabolite 24(S)-hydroxycholesterol is a potent allosteric modulator of N-methyl-D-aspartate receptors. *J Neurosci.* 2013; 33:17290–300. [PubMed: 24174662]

25. Radhakrishnan A, Ikeda Y, Kwon HJ, Brown MS, Goldstein JL. Sterol-regulated transport of SREBPs from endoplasmic reticulum to Golgi: oxysterols block transport by binding to Insig. *Proc Natl Acad Sci U S A*. 2007; 104:6511–18. [PubMed: 17428920]
26. Sodero AO, Vriens J, Ghosh D, et al. Cholesterol loss during glutamate-mediated excitotoxicity. *EMBO J*. 2012; 31:1764–73. [PubMed: 22343944]
27. Noguchi N, Urano Y, Takabe W, Saito Y. New aspects of 24(S)-hydroxycholesterol in modulating neuronal cell death. *Free Radic Biol Med*. 2015; 87:366–72. [PubMed: 26164631]
28. Yamanaka K, Saito Y, Yamamori T, Urano Y, Noguchi N. 24(S)-hydroxycholesterol induces neuronal cell death through necroptosis, a form of programmed necrosis. *J Biol Chem*. 2011; 286:24666–73. [PubMed: 21613228]
29. Alexandrov P, Cui JG, Zhao Y, Lukiw WJ. 24S-hydroxycholesterol induces inflammatory gene expression in primary human neural cells. *Neuroreport*. 2005; 16:909–13. [PubMed: 15931060]
30. Zhao S, Liao W, Xu N, et al. Polar metabolite of cholesterol induces rat cognitive dysfunctions. *Neuroscience*. 2009; 164:398–403. [PubMed: 19699274]
31. Brown J 3rd, Theisler C, Silberman S, et al. Differential expression of cholesterol hydroxylases in Alzheimer's disease. *J Biol Chem*. 2004; 279:34674–81. [PubMed: 15148325]
32. Lavrnja I, Smiljanic K, Savic D, et al. Expression profiles of cholesterol metabolism-related genes are altered during development of experimental autoimmune encephalomyelitis in the rat spinal cord. *Sci Rep*. 2017; 7:2702. [PubMed: 28578430]
33. Liu Y, Silverstein FS, Skoff R, Barks JD. Hypoxic-ischemic oligodendroglial injury in neonatal rat brain. *Pediatr Res*. 2002; 51:25–33. [PubMed: 11756636]
34. Back SA. White matter injury in the preterm infant: pathology and mechanisms. *Acta Neuropathol*. 2017; 134:331–49. [PubMed: 28534077]
35. Silbereis JC, Huang EJ, Back SA, Rowitch DH. Towards improved animal models of neonatal white matter injury associated with cerebral palsy. *Dis Model Mech*. 2010; 3:678–88. [PubMed: 21030421]
36. Funfschilling U, Jockusch WJ, Sivakumar N, et al. Critical time window of neuronal cholesterol synthesis during neurite outgrowth. *J Neurosci*. 2012; 32:7632–45. [PubMed: 22649242]
37. Pfrieger FW, Ungerer N. Cholesterol metabolism in neurons and astrocytes. *Prog Lipid Res*. 2011; 50:357–71. [PubMed: 21741992]
38. Lund EG, Xie C, Kotti T, Turley SD, Dietschy JM, Russell DW. Knockout of the cholesterol 24-hydroxylase gene in mice reveals a brain-specific mechanism of cholesterol turnover. *J Biol Chem*. 2003; 278:22980–8. [PubMed: 12686551]
39. Wu H, Li Z, Yang X, Liu J, Wang W, Liu G. SBDPs and Tau proteins for diagnosis and hypothermia therapy in neonatal hypoxic ischemic encephalopathy. *Exp Ther Med*. 2017; 13:225–9. [PubMed: 28123494]
40. Sheth SA, Iavarone AT, Liebeskind DS, Won SJ, Swanson RA. Targeted Lipid Profiling Discovers Plasma Biomarkers of Acute Brain Injury. *PLoS One*. 2015; 10:e0129735. [PubMed: 26076478]

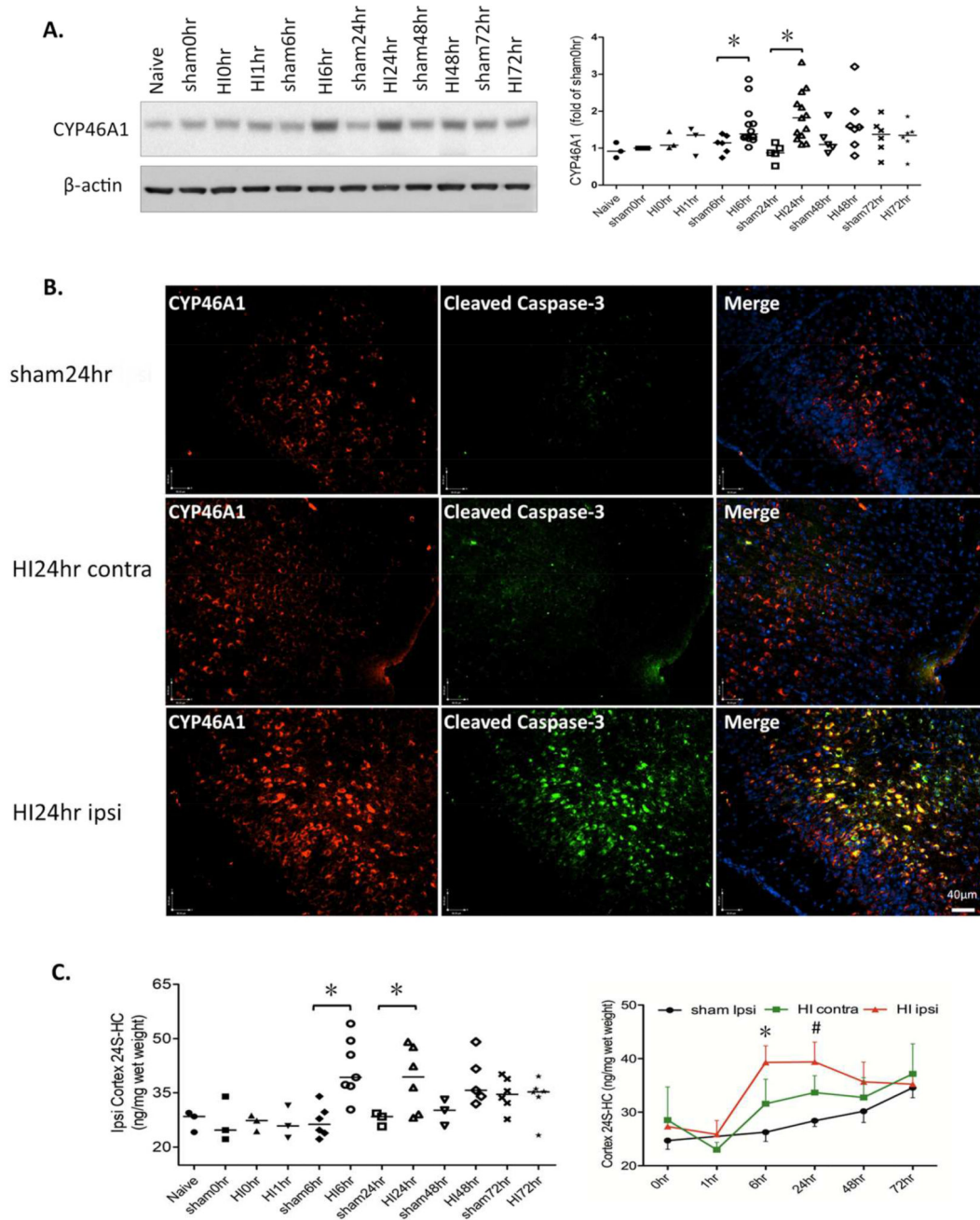


Figure 1.

Up-regulation of CYP46A1 with a concomitant increase of 24S-HC in the ipsilateral cortex after neonatal HI. **A.** Protein expression of CYP46A1 was measured by western blotting at the indicated time points and presented as the OD ratio to β -actin and normalized to the values of sham 0hr (graph on the right, sham vs. HI: * $p=0.0339$ at 6hr; * $p=0.0026$ at 24hr; $n=5-6$ for sham animals, $n=6-12$ for HI animals at 6–72hr). **B.** Immunofluorescent staining with anti-CYP46A1 antibody at 24hr after HI showed enhanced expression in the ipsilateral cortex than that in the contralateral side and in the sham animals (left panels). CYP46A1 staining in the ipsi-cortex was largely co-localized with the expression of cleaved caspase-3

(middle panels). **C.** Increased production of 24S-HC (ng/mg tissue wet weight) in the ipsilateral cortex at 6hr and 24hr after HI (sham vs. HI: * $p=0.0167$ at 6hr; * $p=0.0085$ at 24hr; $n=3-6$ for sham animals, $n=5-7$ for HI animals at 6–72hr). The time course of the changes in 24S-HC in the sham-, contra- and ipsilateral cortex is shown on the right. At 6hr, 24S-HC in the ipsilateral cortex was higher than that in the contralateral side (ipsi- vs. contra-: * $p=0.0493$). #: Significant difference between the HI ipsi- and the sham animals only, but not between the HI ipsi- and HI contralateral hemisphere.

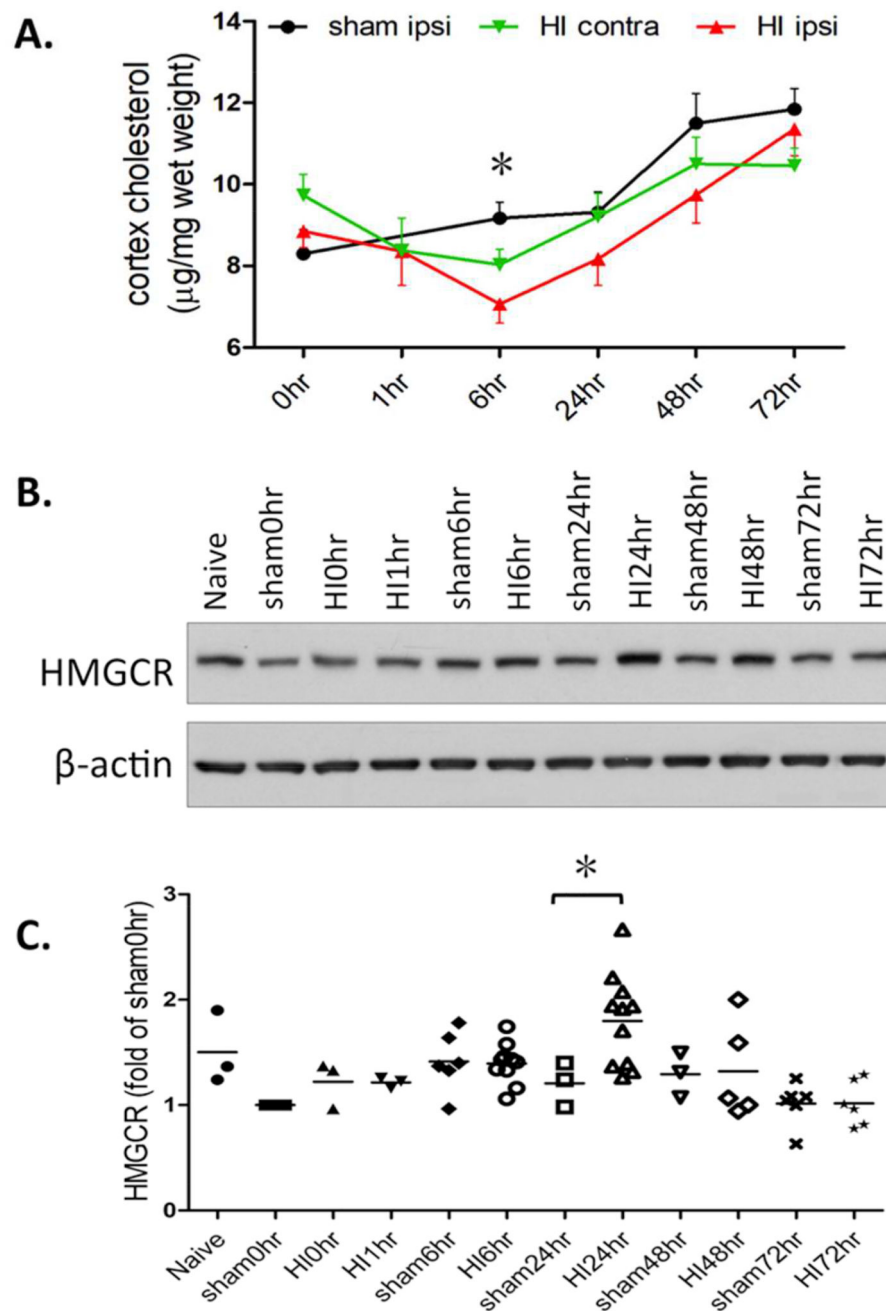
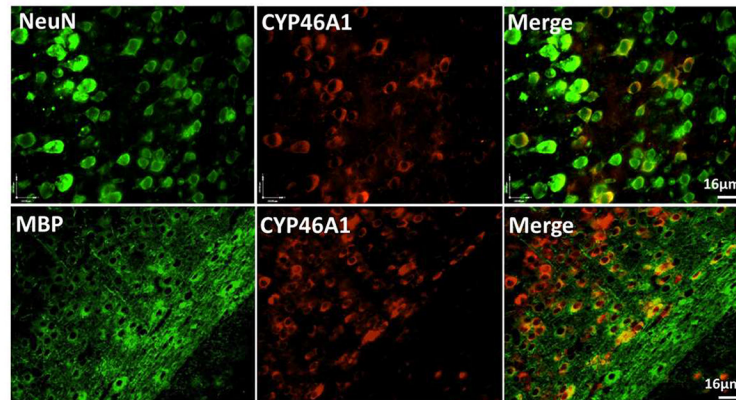
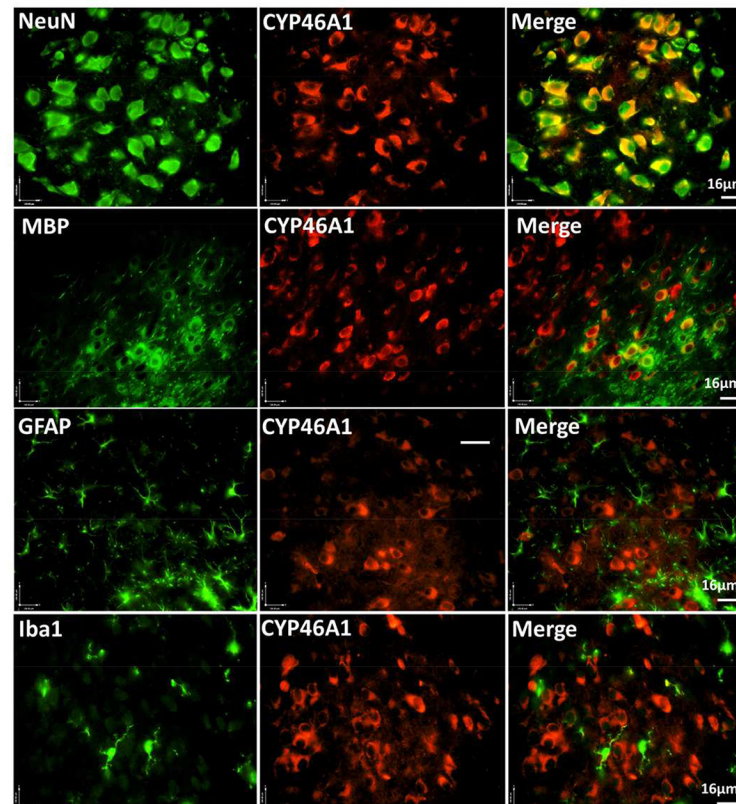


Figure 2. Transient cholesterol loss in the ipsilateral cortex at 6hr after neonatal HI. **A.** The time course of the changes in cholesterol amount in the sham-, contra- and ipsilateral cortex following neonatal HI (sham vs. HI ipsi: * $p=0.0304$ at 6hr; $n=4-7$ for each time points). **B.** Protein expression of HMGCR in the sham and HI-injured cortices was measured by western blotting at the indicated time points. **C.** HMGCR expression is presented as the OD ratio to β -actin and normalized to the values of sham 0hr (sham vs. HI: * $p=0.047$ at 24hr, $n=3-11$).

A: sham24hr



B: HI24hr

**Figure 3.**

Expression of CYP46A1 in the neurons and oligodendrocytes. Images of double Immunofluorescent staining with CYP46A1 antibody (red, middle panels) paired with another antibody specific for neuron (NeuN), oligodendrocyte (MBP), astrocyte (GFAP), or microglia (Iba1), shown in green on the left panels. The representative images from the sham (A) and HI-injured animals at 24hr after HI (B).

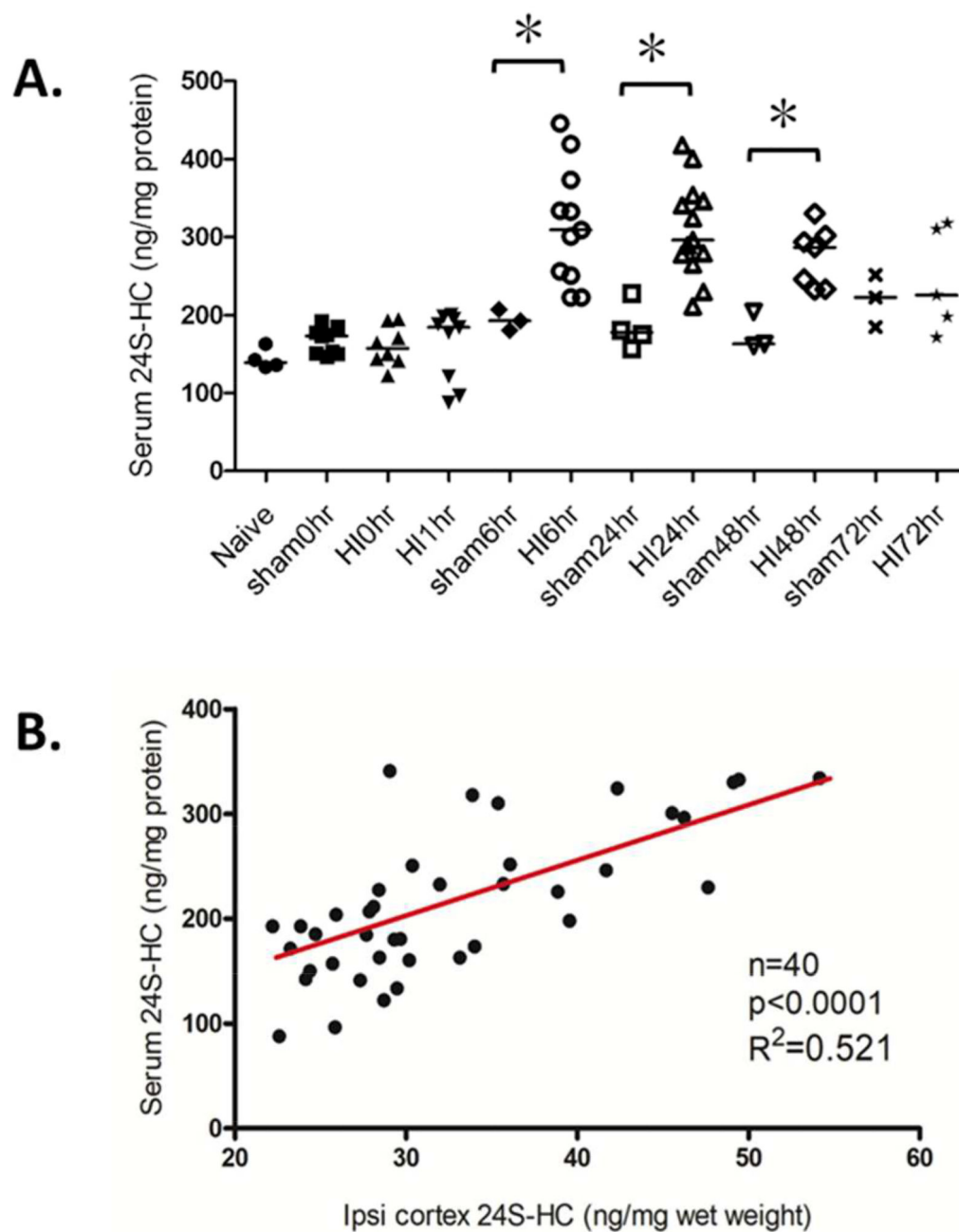
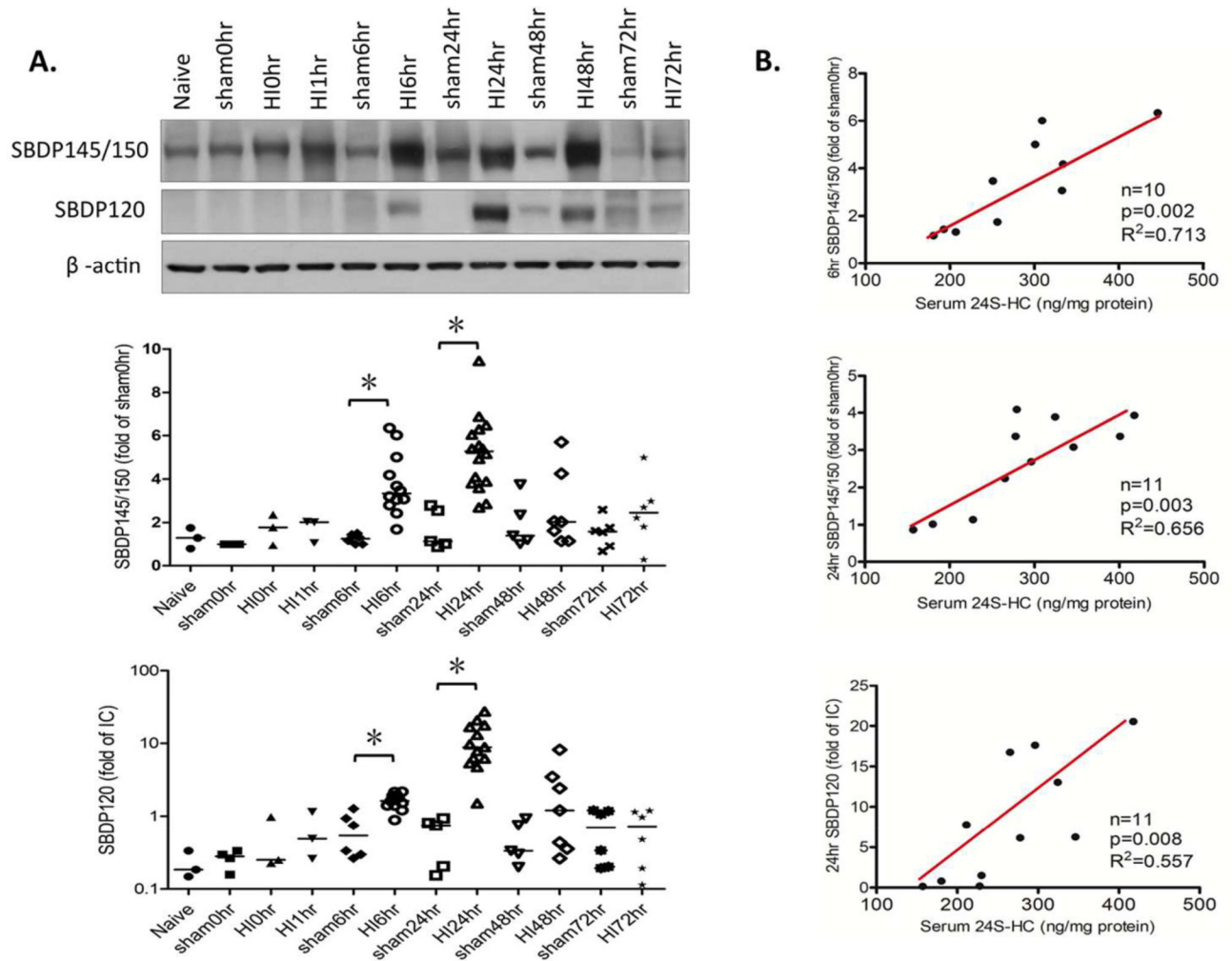


Figure 4. Correlation of the 24S-HC levels in the serum and in the ipsilateral cortex after neonatal HI. **A.** Quantification of the serum levels of 24S-HC (ng/mg serum protein) at the indicated post-HI time points. Sham vs. HI, * $p=0.0102$ at 6hr; * $p=0.0046$ at 24hr; * $p=0.0167$ at 48hr; $n=3-6$ for sham animals, $n=5-13$ for HI animals at 6–72hr. **B.** Correlation of 24S-HC levels in the serum and in the ipsilateral cortex. The samples used in Pearson's correlation coefficient analysis were those included in Fig. 1C. ($n=40$, $R^2=0.521$, $p<0.0001$).

**Figure 5.**

Correlation of the serum levels of 24S-HC with the expression of spectrin breakdown products (SBDP) at 6hr and 24hr after neonatal HI. **A.** Protein expression of SBDP145/150KD and SBDP120KD in the cortices was measured by western blotting at the indicated time points and presented as the OD ratio to β -actin and normalized to the values of sham 0hr (for SBDP145/150), or an internal control (IC, for SBDP120). For SBDP145/150KD, sham vs. HI, *p=0.0094 at 6hr, *p=0.0013 at 24hr. For SBDP120KD, sham vs. HI, *p=0.036 at 6hr, *p=0.0087 at 24hr. (n=4–6 for sham animals, n=6–15 for HI animals from 6–72hr). **B.** Correlation of the serum levels of 24S-HC with the expression of SBDP145/150KD at 6hr (top), at 24hr (middle), and with the expression of SBDP120KD at 24hr (bottom). Sample number, R² and p values are shown in the graphs.

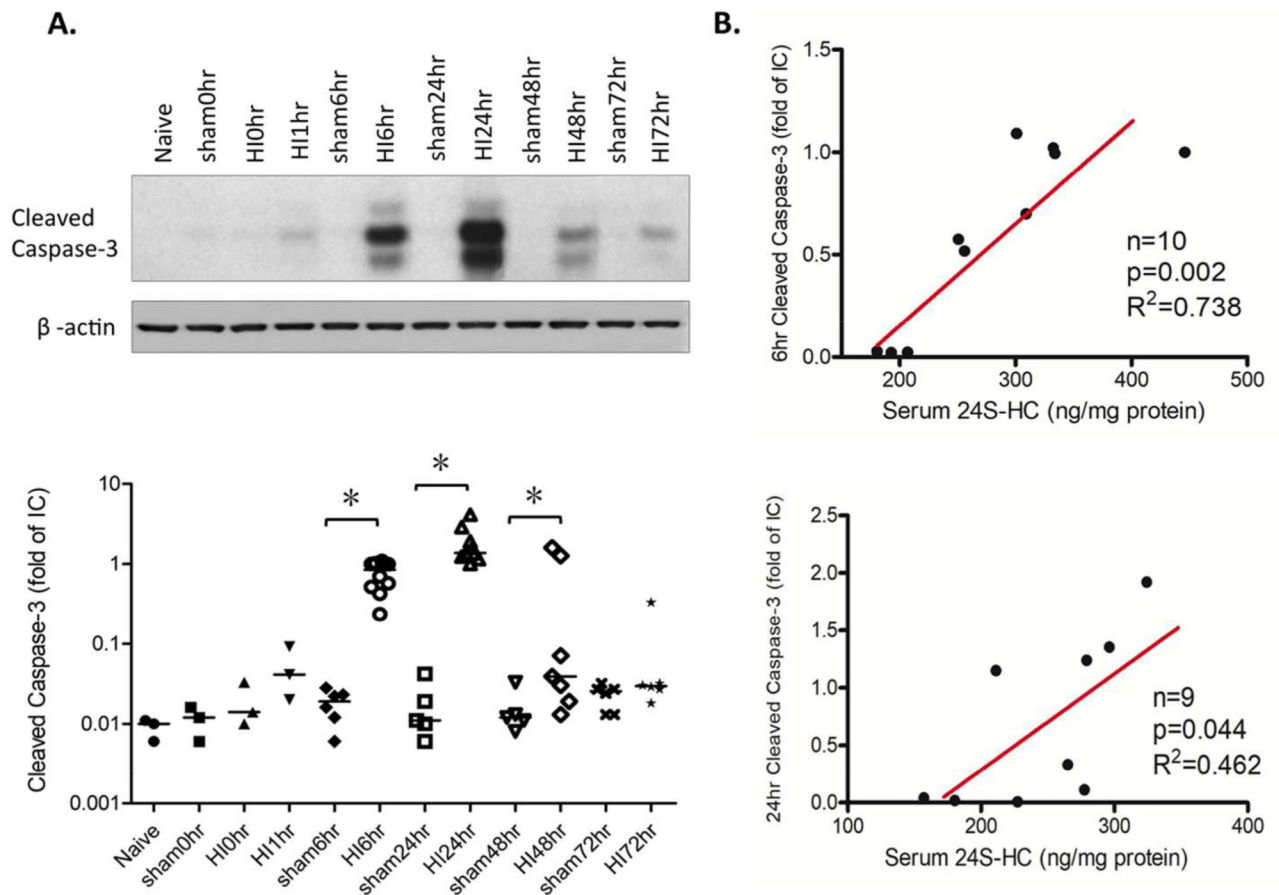


Figure 6.

Correlation of the serum levels of 24S-HC with the expression of cleaved caspase-3 at 6hr and 24hr after neonatal HI. **A.** Protein expression of cleaved caspase-3 in the cortices was measured by western blotting at the indicated time points and presented as the OD ratio to β -actin and normalized to an internal control (IC). Sham vs. HI, * $p=0.0112$ at 6hr; * $p=0.0027$ at 24hr; * $p=0.0228$ at 72hr (n=5–6 for sham animals, n=7–10 for HI animals from 6–72hr).

B. Correlation of the serum levels of 24S-HC with the expression of cleaved caspase-3 at 6hr (top) and at 24hr (bottom). Sample number, R² and p values are shown in the graphs.